ADVANCED METHODS OF ACCELERATION

DESIGN OF A GAS CELL FOR LASER WAKEFIELD ACCELERATION OF ELECTRONS

A.A. Golovanov[1], V.S. Lebedev[1,2], I.Yu. Kostyukov[1]
[1]Institute of Applied Physics RAS, Nizhny Novgorod, Russia;
[2]Lobachevsky State University of Nizhny Novgorod, Nizhny Novgorod, Russia
E-mail: agolovanov@appl.sci-nnov.ru

Laser-wakefield acceleration of electrons in a gas cell is considered. The OpenFOAM package is used to study the influence of the parameters of the cell on the density profile. Particle-in-cell simulations of laser wakefield acceleration are performed for a 150 TW laser pulse, accelerated electrons with energies above 1 GeV are observed. A two-stage gas cell is investigated.

PACS: 52.38.Kd, 47.45.-n

INTRODUCTION

At present, plasma acceleration methods are considered prospective for obtaining high-energy electrons [1, 2]. The main idea of these methods is to use a short laser pulse [3] or a bunch of charged particles [4] to excite a wakefield (a longitudinal plasma wave) in plasma. The electric field in this wave can be used for efficient acceleration, providing acceleration gradients orders of magnitude higher than in conventional radio-frequency linear accelerators.

Nowadays, laser wakefield acceleration (LWFA) in which plasma wakefield is excited by the ponderomotive force of a laser pulse pushing electrons away is one of the main methods of plasma acceleration. The rapid development in the laser technology owing to the invention of the chirped pulse amplification method [5] has led to the emergence of laser facilities capable of generating femtosecond laser pulses with petawatt peak power. The interaction of such intense laser pulses with underdense plasma is so strong that the plasma wave is excited in the strongly non-linear ("bubble") regime. In this regime, the laser pulse expels almost all electrons from the axis of its propagation, leading to the formation of a spherical cavity free of plasma electrons [6]. This cavity is often referred to as a bubble.

The bubble regime is of particular interest for laser wakefield acceleration because it allows for self-injection of plasma electrons: electrons from the background plasma can be trapped and accelerated in the bubble [7]. Self-injection makes the experimental realization of LWFA much easier, as no external electron source synchronized with the laser system is required. The simplest experimental setup includes a supersonic gas jet and a femtosecond laser system. The laser pulse generated by this system interacts with the gas jet, fully ionizing the gas and generating a bubble in the resulting plasma. Plasma electrons are trapped and accelerated in the bubble, resulting in an accelerated electron bunch. Such an electron bunch can have energies of hundreds of MeVs and a relatively small energy spread if the parameters of the laser pulse are properly tailored to the plasma density [8 - 10].

However, the stability, the maximum obtainable energy and the quality of the accelerated bunch are lacking in such a simple scheme, and many alternative approaches are proposed. One of them revolves around using a controlled plasma profile. Unlike a gas jet, in which plasma is significantly non-uniform and only few parameters controlling the profile exist, a controlled plasma profile can be optimized for specific tasks. At the moment, the highest energy of the accelerated electrons equal to 4.2 GeV has been demonstrated for acceleration in a 9-cm-long capillary in which plasma with near-parabolic transverse profile has been created by a discharge [11]. Such a transverse plasma profile is used to guide the laser pulse. However, tailoring the longitudinal (along the laser propagation) plasma profile is also of interest. One of the improved gas targets with a controllable longitudinal profile are gas cells [12, 13]. A simple gas cell consists of a closed volume filled with gas with an inlet for pumping the gas into it and two small outlets on its side through which a laser pulse can enter and exit the cell. Some of the gas inevitably leaks into the vacuum outside the cell through these outlets. Gas density is uniform inside the cell, which can be used to create a several-cm-long uniform plasma profile of specified density. More advanced types of gas cells with two stages can also be used for different injection techniques [14 - 16].

As experiments with LWFA are costly, and interpreting their results is difficult, numerical simulations play a big role in studying the physics of laser-plasma interactions. The most general method for self-consistent simulation of plasmas and the electromagnetic field is the particle-in-cell (PIC) method [17]. This method relies on solving the Maxwell's equations for the fields and equations of motion for macroparticles consisting of a large number of real particles in the three-dimensional space. As it is based on fundamental physical laws, it can be used for a wide range of problems and can often provide results similar to the experimental ones, which warrants its use as a tool for "numeric experiments".

However, in order to properly model LWFA in a gas cell, it is necessary to know the density profile of gas in the cell beforehand. Direct measurements in experimentally realized gas cells pose difficulties and also limit the freedom of choice of gas cell parameters. Alternatively, computational fluid dynamics (CFD) methods can be used to calculate the distribution of the gas density. Such CFD simulations for simple two- and three-dimensional models of a gas cell and their application to PIC simulations of LWFA are considered in this paper.

In Sec. 2, a simple model of a gas cell is presented, and the influence of the gas cell parameters on the density profile is studied. In Sec. 3, PIC simulations of LWFA based on one of the calculated profiles are described. Finally, in Sec. 4, a more advanced two-stage gas cell is considered and the possibility of creating a density profile with two plateaus is discussed.

1. GAS CELL SIMULATIONS

Simulations of a gas cell were performed using the open-source CFD package OpenFOAM [18, 19]. The standard sonicFoam solver from this package was chosen to simulate the supersonic gas flow in the cell. In most simulations, we used two-dimensional gas cell models which allowed us to significantly decrease the computation time while leaving it possible to study the problem qualitatively. The basic two-dimensional model of a single-chamber gas cell is shown in Fig. 1. It consists of the main volume of the gas cell, the inlet at the top through which gas enters the cell, and two outlets at its left and right sides through which the gas leaves the cell. A laser pulse can pass through the cell through the outlets along the dashed line in Fig. 1. The semicircles are used to simulate vacuum outside the gas cell; boundary conditions on them allow for gas outflow without reflections. Both the model and the numerical mesh for this model were created using *gmsh* [20, 21].

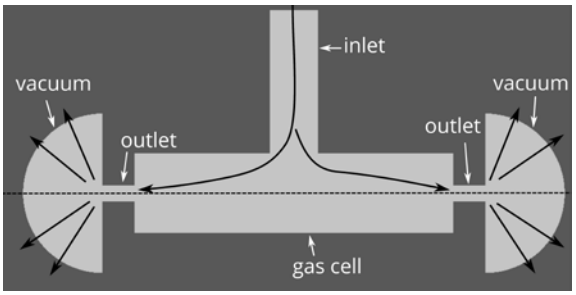

Fig. 1. A schematic of a two-dimensional gas cell. Arrows show the gas flow in the cell. The dashed line shows the axis along which a laser pulse propagates through the cell

In the simulations, we used helium at the temperature of 300 K and the pressure at the inlet of 8 kPa corresponding to the expected mass density of 12.8 g/m^3. Initially, the cell was nearly empty (at 0.2 kPa), and the pressure at the inlet was linearly raised to 8 kPa over the course of 100 μs. The flow usually reached a near-steady state in less than 1 ms. Turbulence was taken into account using the *k-ω* SST model [22, 23] available in OpenFOAM. Accounting for turbulence is important as it significantly improves the convergence rate to the steady state due to the increased viscosity and thermal conductivity, but it does not influence the end result of the gas density distribution. The gas cell was 20 mm long and 5 mm wide, the sizes (widths) of the inlet and the outlets were 3 mm and 1 mm, respectively. The resulting gas density profile on the axis of the cell (the dashed line in Fig. 1) is shown in Fig. 2,a. Inside the cell, the density is mostly uniform, and it rapidly drops to zero as the gas leaves the cell through the outlets into vacuum. The resulting level is slightly lower than the equilibrium density level at 8 kPa due to the constant flow of gas through the cell.

The simple model in Fig. 1 allowed us to better understand which parameters of the gas cell are important for the resulting density profile on its axis. In order to do that, we performed a series of simulations with various parameters of the cell. First, we varied the transverse and the longitudinal sizes of the cell. The transverse size did not change the density profile in any significant way, which means that it can be arbitrary chosen according to the manufacturing and ease-of-use constraints. At the same time, the length of the cell can be used to effectively change the length of the plateau in the density profile, as shown in Fig. 2,b.

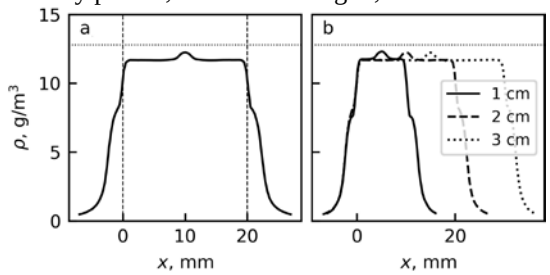

Fig. 2. (a) Gas density profile ρ(x) on the axis of the cell in Fig. 1. The vertical dashed lines show the boundaries of the cell. The horizontal dotted line shows the expected density at the pressure of 8 kPa and the temperature of 300 K. (b) Gas density profiles for different lengths of the cell (1, 2, 3 cm)

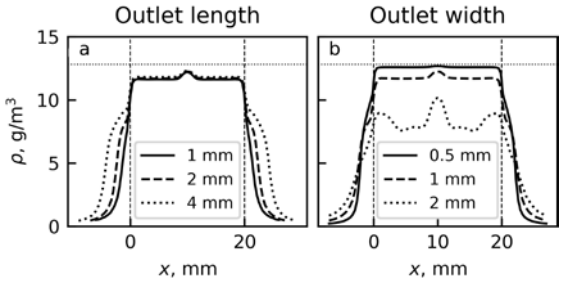

Fig. 3. Gas cell density profiles for (a) different lengths of the outlets (1, 2, 4 mm), (b) different widths of the outlets (0.5, 1, 2 mm) for the inlet width of 3 mm. The vertical dashed lines show the boundaries of the cell. The horizontal dotted lines show the expected density at the pressure of 8 kPa and the temperature of 300 K

The second major feature of a gas cell are the presence of the inlet and the outlets. As our simulations showed, their positions (e.g., the inlet being at the center or closer to the left boundary) are not very important. The same applies to the length of the inlet, while the lengths of the outlets modify the distance at which the density drops to zero (Fig. 3,a), so it is preferable to make outlets as short as possible. Typically, their length is equal to the thickness of the gas cell walls. However, the most important characteristic is the ratio of the total cross-section of the outlets to the total cross-section of the inlet (or several inlets if there are many). For example, in our case, if the inlet's size is 3 mm, and the outlets are 1 mm each, this ratio is (1+1)/3=2/3. As Fig. 3,b shows, when this ratio is smaller than 1, the density profile is mostly uniform with the peak density close to the expected density at the specified pressure. However, when this ratio exceeds 1, the inlet can no longer maintain the desired density, as the gas quickly leaves the cell. The flow of the gas inside the cell becomes highly

turbulent, and the density profile becomes non-uniform and non-stationary (the profile shown in Fig. 3,b is a snapshot at one time moment). Therefore, it is desirable to make outlets as small as possible and to increase the size of the inlet. In practice, the size of the outlets is limited by the ability to robustly focus the laser pulse onto them, as it may possibly damage the walls of the cell if not focused properly.

It is also important to estimate the total mass flow through the outlets to determine the requirements to maintaining vacuum conditions in the experimental vacuum chamber. A simple upper boundary for the mass flow can be given using the model of gas expansion into vacuum, where the expected gas density is multiplied by the thermal velocity:

$$\frac{\mathrm{d}m}{\mathrm{d}S\,\mathrm{d}t} = \rho v_T \approx 17.5\,\mathrm{kg/(m^2 \cdot s)}. \qquad (1)$$

In reality, however, the mass flow should be lower, as the gas-vacuum boundary is not abrupt. The observed mass flow in the simulations corresponding to Fig. 2 was equal to 5.5 kg/(m^2·s).

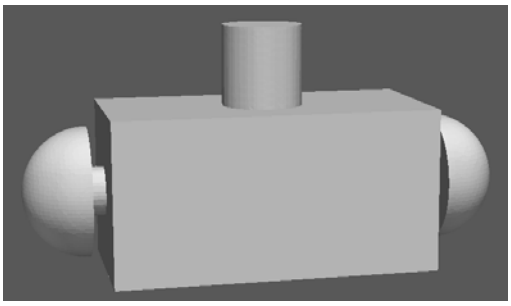

Fig. 4. A three-dimensional model of a gas cell

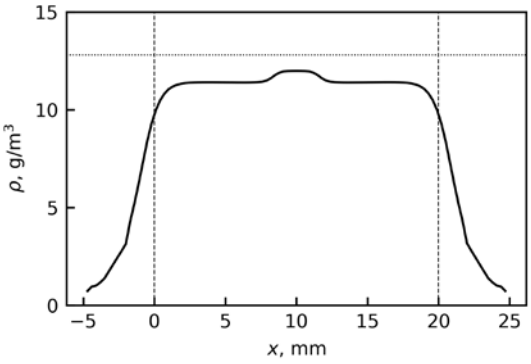

Fig. 5. Gas density profile on the axis of the three-dimensional gas cell shown in Fig. 4

Similar simulations have been performed in the 3D geometry using the model shown in Fig. 4. The model is similar to the 2D model in Fig. 1 and has one inlet at the top and two side outlets. The gas profile on the axis of such a cell is shown in Fig. 5. In general, the observed properties of the density profile are the same as in the two-dimensional case. It is uniform inside the gas cell and drops to zero outside the cell. However, the rate at which the density drops to zero is different in the 3D and 2D geometries. In the 3D case, the front of the expanding gas is a sphere, and the density in the vacuum drops as $1/r^2$ with the distance from the cell. This rate is higher than the $1/r$ rate in the 2D case. Overall, the comparison shows that the two-dimensional geometry is suitable for making qualitative conclusions about gas cells.

2. PIC SIMULATIONS

In order to demonstrate the use of a gas cell for laser wakefield acceleration, we performed simulations using the 3D particle-in-cell (PIC) code Quill [24, 25]. In the simulations, we used a 9 J, 60 fs Gaussian laser pulse with the wavelength of 910 nm corresponding to the parameters attainable at the laser complex PEARL [26]. The peak power of such a pulse reached 145 TW. The pulse was assumed to be focused by a f/40 mirror with the spot size of 30 μm. Such a laser pulse fully ionized helium by its front already, and thus the number density of electrons in the PIC simulations was simply two times larger than the number density of helium in the OpenFOAM simulations of the cell. The discretized mass density of helium on the gas cell axis from the OpenFOAM simulations was exported to a CSV file and transformed by a script into the number density of electrons which was read by the PIC code. By linear interpolation of the read discretized values, a longitudinal profile of plasma was recreated. A 17-mm long single-chamber gas cell was used in the OpenFOAM simulations. The pressure of 8 kPa used in the simulations corresponded to the electron number density in plasma of 3.85×10^{18} cm^{-3}.

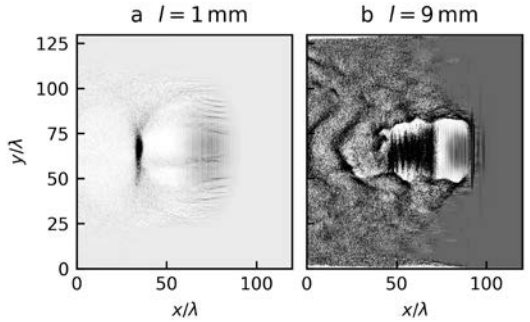

Fig. 6. Wakefield excited by a laser pulse after propagating for (a) 1 mm and (b) 9 mm. The pulse is propagating to the right

Initially, when the density outside the gas cell is still small (Fig. 6,a), the interaction of the laser pulse with the plasma is weak, and no electrons are trapped. As the laser pulse enters the denser plasma inside the cell (Fig. 6,b), self-focusing leads to its contraction and the increase of the peak power. A bubble is formed behind the laser pulse, and electrons are trapped into it. The trapped electron bunch is visible in Fig. 6,b.

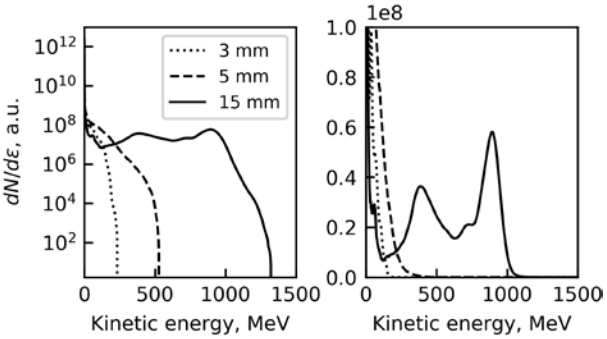

Fig. 7. Spectra of accelerated electrons in the logarithmic (left) and linear (right) scales for different distances (3, 5, and 15 mm) of the laser pulse propagation

Spectra of accelerated electrons for different distances of the laser pulse propagation are shown in Fig. 7. As the pulse enters the cell and propagates in it, more electrons are trapped leading to the increase of the total charge. At the same time, the maximum electron energy grows rapidly, reaching the values beyond 1 GeV. Higher energies for the considered parameters cannot be reached as the laser pulse begins to deplete.

3. TWO-STAGE GAS CELL

As shown in Sec. 2, simple gas cells can be used to create uniform gas density profile which is desirable for laser-plasma acceleration. However, more complex profiles might be of interest. For example, a profile with two plateaus of different levels might be useful. A model of a gas cell capable of providing such a profile is shown in Fig. 8. It consists of two volumes (chambers) connected by a small hole. Each volume has its own inlet to control the pressure inside the volume. The resulting gas density profile can be used in the following way. The first short part with denser plasma is used as an injector in which plasma electrons are trapped into a bubble via self-injection [7]. However, the maximum attainable energy is inversely proportional to the plasma density, so it might be desirable to accelerate electrons in a less dense gas. Therefore, the second (longer) chamber should have a lower density. In addition, this density might be below the self-injection threshold, which means that no new electrons will be trapped and the accelerated bunch will remain quasimonoenergetic.

Fig. 8. A model of a two-stage gas cell

In the design of a two-chamber gas cell, it is important to understand how large the ratio between the densities in the two chambers can be. Obviously, as they are connected, the gas will flow from the chamber with the higher pressure into the chamber with the lower pressure, and thus the pressure in the second chamber cannot be infinitely small. In order to determine the lowest possible pressure, the inlet in the second cell might be sealed, so that the only source of gas in it is its connection to the first chamber. In simulations, it is emulated by changing the boundary conditions on the inlet to the wall boundary conditions. The results of such simulations for different sizes of the hole between the chambers are shown in Fig. 9,a. When the hole is much smaller that the size of the outlets (the solid line, a 0.2 mm hole and 1 mm outlets), the density level inside the second cell is much lower than in the first cell, as the gas leaves the second chamber much faster than enters it. However, in the opposite case (the dotted line, a 2 mm hole and 1 mm outlets), the gas cannot leave the second cell fast enough, and the cell effectively becomes similar a single-chamber one. Therefore, it is extremely important that the size of the hole between two chambers is made as small as possible. When this condition is satisfied, the density levels in two chambers can be controlled independently, as shown in Fig. 9,b for the pressures at the two inlets of 8 and 4 kPa, respectively.

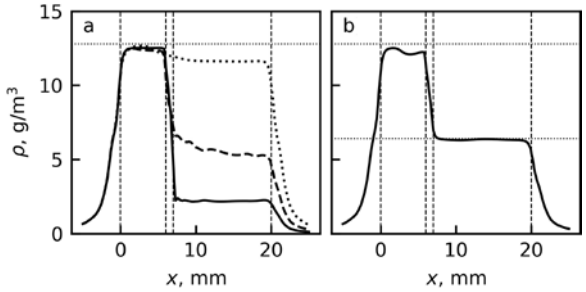

Fig. 9. (a) Gas density profiles in a two-stage cell without the second inlet for different sizes of the hole between the two chambers. The solid, dashed, and dotted lines correspond to the sizes of 0.2, 0.5, 2 mm, respectively. The size of the outlets is 1 mm. (b) Gas density profile in a two-stage cell for the pressure at the first and the second inlets of 8 kPa and 4 kPa, respectively. The size of the outlet is 1 mm, the size of the hole between the chamber is 0.2 mm. The horizontal dotted lines show the expected density levels at these two pressures. The vertical dashed lines show the boundaries of the cells

CONCLUSIONS

Specifically tailored plasma density distribution can be used to improve laser wakefield acceleration of electrons. In this paper, gas cells were considered as one of the methods of creating longitudinal plasma profiles with long uniform plateaus. In order to investigate the influence of the gas cell parameters on the gas density distribution inside it, numerical CFD simulations with the open-source OpenFOAM package were performed. In these simulations, we considered a simple two-dimensional model of a gas cell and showed that the profile of the gas in such a cell is quasistationary and uniform if the size of the outlets is small enough. Three-dimensional simulations confirmed our findings. Using one of the resulting profiles, particle-in-cell simulations of the laser wakefield acceleration were performed with the 3D PIC code Quill. The simulations showed that accelerated electrons with the energy above 1 GeV can be obtained in such a gas cell. In addition, a two-stage gas cell capable of creating two different-level plateaus in the gas density was considered. It was shown that such a profile can be realized if the hole connecting the two chambers is small enough.

Gas cell computation has been supported by the Russian Foundation for Basic Research through Grant № 18-32-00943 (A.A.G. and V.S.L.). Simulations of electron acceleration have been supported by the Russian Science Foundation through Grant № 16-12-10383 (I.Yu.K.).

REFERENCES

1. E. Esarey, C. Schroeder, W. Leemans. Physics of laser-driven plasma-based electron accelerators // *Review of Modern Physics (81).* 2014, № 3, p. 1229.

2. I.Yu. Kostyukov, A.M. Pukhov. Plasma-based methods for electron acceleration: current status and prospects // *Physics-Uspekhi (58).* 2015, № 1, p. 81.
3. T. Tajima, J.M. Dawson. Laser electron accelerator // *Physical Review Letters (43).* 1979, № 4, p. 267.
4. J.B. Rosenzweig, D.B. Cline, B. Cole, H. Figueroa, W. Gai, R. Konecny, J. Norem, P. Schoessow, J. Simpson. Experimental observation of plasma wake-field acceleration // *Physical Review Letters (61).* 1988, № 1, p. 98.
5. D. Strickland, G. Mourou. Compression of amplified chirped optical pulses // *Optics Communications (56).* 1985, № 3, p.219.
6. A. Pukhov, J. Meyer-ter-Vehn. Laser wake field acceleration: the highly non-linear broken-wave regime // *Applied Physics B: Lasers and Optics (74).* 2002, № 4-5, p. 355-361.
7. D.H. Froula, C.E. Clayton, T. Döppner, K.A. Marsh, C.P.J. Barty, L. Divol, R.A. Fonseca, S.H. Glenzer, C. Joshi, W. Lu, S.F. Martins, P. Michel, W.B. Mori, J.P. Palastro, B.B. Pollock, A. Pak, J.E. Ralph, J.S. Ross, C.W. Siders, L.O. Silva, T. Wang. Measurements of the critical power for self-injection of electrons in a laser wakefield accelerator // *Physical Review Letters (103).* 2009, № 21, p. 215006.
8. C.G.R. Geddes, Cs. Toth, J. van Tilborg, E. Esarey, C.B. Schroeder, D. Bruhwiler, C. Nieter, J. Cary, W.P. Leemans. High-quality electron beams from a laser wakefield accelerator using plasma-channel guiding // *Nature (431).* 2004, № 7008, p. 538.
9. S.P.D. Mangles, C.D. Murphy, Z. Najmudin, A.G.R. Thomas, J.L. Collier, A.E. Dangor, E.J. Divall, P.S. Foster, J.G. Gallacher, C.J. Hooker, D.A. Jaroszynski, A.J. Langley, W.B. Mori, P.A. Norreys, F.S. Tsung, R. Viskup, B.R. Walton, K. Krushelnick. Monoenergetic beams of relativistic electrons from intense laser-plasma interactions // *Nature (431).* 2004, № 7008, p. 535.
10. J. Faure, Y. Glinec, A. Pukhov, S. Kiselev, S. Gordienko, E. Lefebvre, J.-P. Rousseau, F. Burgy, V. Malka. A laser–plasma accelerator producing monoenergetic electron beams // *Nature (431).* 2004, № 7008, p. 541.
11. W.P. Leemans, A.J. Gonsalves, H.-S. Mao, K. Nakamura, C. Benedetti, C.B. Schroeder, Cs. Tóth, J. Daniels, D.E. Mittelberger, S.S. Bulanov, J.-L. Vay, C.G.R. Geddes, E. Esarey. Multi-GeV electron beams from capillary-discharge-guided subpetawatt laser pulses in the self-trapping regime // *Physical Review Letters (113).* 2014, № 24, p. 245002.
12. J. Osterhoff, A. Popp, Zs. Major, B. Marx, T. Rowlands-Rees, M. Fuchs, M. Geissler, R. Hörlein, B. Hidding, S. Becker, E. Peralta, U. Schramm, F. Grüner, D. Habs, F. Krausz, S. Hooker, S. Karsch. Generation of stable, low-divergence electron beams by laser-wakefield acceleration in a steady-state-flow gas cell // *Physical Review Letters (101).* 2008, № 8, p. 085002.
13. C.E. Clayton, J.E. Ralph, F. Albert, R.A. Fonseca, S.H. Glenzer, C. Joshi, W. Lu, K.A. Marsh, S.F. Martins, W.B. Mori, A. Pak, F.S. Tsung, B.B. Pollock, J.S. Ross, L.O. Silva, D.H. Froula. Self-guided laser wakefield acceleration beyond 1 GeV using ionization-induced injection // *Physical Review Letters (105).* 2010, № 10, p. 105003.
14. B.B. Pollock, C.E. Clayton, J.E. Ralph, F. Albert, A. Davidson, L. Divol, C. Filip, S.H. Glenzer, K. Herpoldt, W. Lu, K.A. Marsh, J. Meinecke, W.B. Mori, A. Pak, T.C. Rensink, J.S. Ross, J. Shaw, G.R. Tynan, C. Joshi, D.H. Froula. Demonstration of a narrow energy spread, ~0.5 GeV electron beam from a two-stage laser wakefield accelerator // *Physical Review Letters (107).* 2011, № 4, p. 045001.
15. M. Vargas, W. Schumaker, Z.-H. He, Z. Zhao, K. Behm, V. Chvykov, B. Hou, K. Krushelnick, A. Maksimchuk, V. Yanovsky, A.G.R. Thomas. Improvements to laser wakefield accelerated electron beam stability, divergence, and energy spread using three-dimensional printed two-stage gas cell targets // *Applied Physics Letters (104).* 2014, № 17, p. 174103.
16. O. Kononenko, N.C. Lopes, J.M. Cole, C. Kamperidis, S.P.D. Mangles, Z. Najmudin, J. Osterhoff, K. Poder, D. Rusby, D.R. Symes, J. Warwick, J.C. Wood, C.A.J. Palmer. 2D hydrodynamic simulations of a variable length gas target for density down-ramp injection of electrons into a laser wakefield accelerator // *Nuclear Instruments and Methods in Physics Research Section A: Accelerators, Spectrometers, Detectors and Associated Equipment (829).* 2016, p. 125-129.
17. A. Pukhov. Particle-in-cell codes for plasma-based particle acceleration // *CERN Yellow Reports (1).* 2016, p. 181.
18. H. Jasak. OpenFOAM: Open source CFD in research and industry // *International Journal of Naval Architecture and Ocean Engineering (1).* 2009, № 2, p. 89-94.
19. https://www.openfoam.com/
20. C. Geuzaine, J. Remacle. Gmsh: A 3-D finite element mesh generator with built-in pre- and post-processing facilities // *International Journal for Numerical Methods in Engineering (79).* 2009, № 11, p. 1309-1331.
21. http://gmsh.info/
22. F.R. Menter. Two-equation eddy-viscosity turbulence models for engineering applications // *AIAA Journal (32).* 1994, № 8, p. 1598-1605.
23. F.R. Menter, M. Kuntz, R. Langtry. Ten years of industrial experience with the SST turbulence model // *Proceedings of the fourth international symposium on turbulence, heat and mass transfer.* 2003, p. 625-632.
24. E.N. Nerush, I.Yu. Kostyukov. Modelling of QED effects in superstrong laser field // *Problems of Atomic Science and Technology (4).* 2010, p. 3-7.
25. http://iapras.ru/english/structure/dep_330/quill.html
26. V.V. Lozhkarev, G.I. Freidman, V.N. Ginzburg, E.V. Katin, E.A. Khazanov, A.V. Kirsanov, G.A. Luchinin, A.N. Mal'shakov, M.A. Martyanov, O.V. Palashov, A.K. Poteomkin, A.M. Sergeev, A.A. Shaykin, I.V. Yakovlev. Compact 0.56 petawatt laser system based on optical parametric chirped pulse amplification in KD*P crystals // *Laser Physics Letters (4).* 2007, № 6, p. 421.

Article received 31.05.2018

РАЗРАБОТКА ГАЗОВОЙ ЯЧЕЙКИ ДЛЯ ЛАЗЕРНО-ПЛАЗМЕННОГО УСКОРЕНИЯ ЭЛЕКТРОНОВ

А.А. Голованов, В.С. Лебедев, И.Ю. Костюков

Рассмотрено лазерно-плазменное ускорение электронов в газовой ячейке. При помощи пакета OpenFOAM исследовано влияние параметров ячейки на профиль плотности. Проведено моделирование методом «частиц в ячейках» лазерно-плазменного ускорения для лазерного импульса мощностью 150 ТВт, при этом наблюдались ускоренные электроны с энергией более 1 ГэВ. Исследована двухстадийная газовая ячейка.

РОЗРОБКА ГАЗОВОЇ КОМІРКИ ДЛЯ ЛАЗЕРНО-ПЛАЗМОВОГО ПРИСКОРЕННЯ ЕЛЕКТРОНІВ

А.А. Голованов, В.С. Лебедев, И.Ю. Костюков

Розглянуто лазерно-плазмове прискорення електронів у газовій комірці. За допомогою пакета OpenFOAM досліджено вплив параметрів середовища на профіль густини. Проведено моделювання методом «частинок у комірці» лазерно-плазмового прискорення для лазерного імпульсу потужністю 150 ТВт, при цьому спостерігалися прискорені електрони з енергією більше 1 ГеВ. Досліджена двостадійна газова комірка.